Journal of Neuropathology and Experimental Neurology

Vol. 58, No. 6
June, 1999
pp. 667–677

Frontotemporal Dementia and Corticobasal Degeneration in a Family with a P301S Mutation in *Tau*

ORSO BUGIANI, MD, JILL R. MURRELL, PHD, GIORGIO GIACCONE, MD, MASATO HASEGAWA, PHD, GIUSEPPE GHIGO, MD, MASSIMO TABATON, MD, MICHELA MORBIN, MD, ALBERTO PRIMAVERA, MD, FRANCESCO CARELLA, MD, CLAUDIO SOLARO, MD, MARINA GRISOLI, MD, MARIO SAVOIARDO, MD, MARIA GRAZIA SPILLANTINI, PHD, FABRIZIO TAGLIAVINI, MD, MICHEL GOEDERT, MD, PHD, AND BERNARDINO GHETTI, MD

Abstract. The tau gene has been found to be the locus of dementia with rigidity linked to chromosome 17. Exonic and intronic mutations have been described in a number of families. Here we describe a P301S mutation in exon 10 of the tau gene in a new family. Two members of this family were affected. One individual presented with frontotemporal dementia, whereas his son has corticobasal degeneration, demonstrating that the same primary gene defect in tau can lead to 2 distinct clinical phenotypes. Both individuals developed rapidly progressive disease in the third decade. Neuropathologically, the father presented with an extensive filamentous pathology made of hyperphosphorylated tau protein. Biochemically, recombinant tau protein with the P301S mutation showed a greatly reduced ability to promote microtubule assembly.

Key Words: Cytoskeleton; Dementia; Mutation; Neurodegenerative Disease; Tau proteins.

INTRODUCTION

The question has been raised whether frontotemporal dementia (FTD) and corticobasal degeneration (CBD) are distinct entities (1). An answer to this question is relevant to the nosography of sporadic and familial diseases with focal degeneration of the telencephalon (also referred to as lobar atrophies). They include FTD, frontal atrophy with motor neuron disease, progressive aphasia, CBD, progressive subcortical gliosis, and thalamo-striatal dementia (2).

Symptoms and gross pathology point to FTD and CBD as separate entities. Most FTD patients suffer from emotional and behavioral difficulties with intellectual and motor decline resulting in dementia and rigidity (3). Familial FTD with parkinsonism (rigidity is often referred to as parkinsonism) is linked to chromosome 17 (FTDP-17) (3–5) and is associated with mutations in the tau gene (6–12). Under normal conditions, tau protein promotes the assembly of microtubules and binds to microtubules that are stabilized in the process. It also makes up the cytoskeletal pathology that underlies several neurodegenerative diseases (13). In contrast to patients with FTD, CBD patients present with a dystonic limb (most often a hand) progressing to rigidity with abnormal movements and cortical sensory loss. They are intellectually unaffected until the late stages of the disease (14). A familial occurrence of CBD has been reported (15). Clinical differences between FTD and CBD have a correlate in the distribution of cerebral atrophy, as detected by MRI during life. In FTD, gray and white matter of the frontal and/or temporal lobes and frequently the caudate nuclei are severely (sometimes asymmetrically) affected. Atrophy in CBD is asymmetrical, with one parietal lobe being more affected than the other, often with adjacent frontal areas also being atrophic.

Despite these differences, FTD and CBD share a filamentous cytoskeletal pathology made of hyperphosphorylated tau protein within affected neurons and glial cells. This paper reports on 2 patients, father and son, presenting with FTD and CBD, respectively, and carrying a P301S mutation in exon 10 of the tau gene. This finding demonstrates that either FTD or CBD can be caused by the same primary gene defect.

MATERIAL AND METHODS

Pedigree

Two members (II-1 and III-2) of family P (Fig. 1), who lived in the same house and were employed at the same nursing home, developed neurological symptoms when in their late 20s. Members of the first generation were healthy, as are relatives of the second and third generation now in their 60s and 30s, respectively. Members of the fourth generation are still below the age of onset of the disease in II-1 and III-2. All the members of this pedigree were examined by one of us (OB).

Patients

Patient II-1: At age 29 this patient started to complain of depressive mood, memory loss, and difficulty concentrating. Two years later a neurological examination disclosed grasp reflex and brisk tendon reflexes, slight rigidity, moderate defects of spoken expression, severe

From the Istituto Neurologico Carlo Besta, Milano, Italy (OB, GG, MM, FC, MGr, MS, FT); Laboratory of Molecular Neuropathology, Indiana University School of Medicine, Indianapolis, Indiana, (JRM, BG); Ospedale Psichiatrico (GGh) and Dipartimento di Neuroscienze dell'Università, Genova, Italy (MT, AP, CS); Medical Research Council, Laboratory of Molecular Biology, (MH, MG) and Department of Neurology, University of Cambridge (MGS), Cambridge, United Kingdom.

Grant Support from the Italian Ministry of Public Health, the UK Medical Research Council, the Royal Society of London, and the US Public Health Service grants AG10133, NS14426 (BG), and NS37431 (JRM).

Correspondence to: Orso Bugiani, MD, Istituto Neurologico Carlo Besta, via Celoria 11, 20133 Milano MI, Italy.

memory loss, and inappropriate behavior. Subsequently, he was reportedly apathetic, indifferent, and self-neglectful, while manifesting occasional visual and auditory hallucinations, as well as persecutory delusions. He was diagnosed as schizophrenic and admitted to a nursing home. As the disease progressed he became more and more withdrawn, disoriented, unable to communicate, and in the last year of his life he was rigid and bedridden. Death occurred at 36 yr of age.

Patient III-2, Son of II-1: At age 27 this patient became aware of odd positioning and awkward movements of his left hand. In 3 yr these symptoms evolved to rigidity and dystonia with fingers kept slightly flexed. He had also lost the ability to recognize finger position and to localize tactile stimulation in the left hand. As the dystonic rigidity progressed, the left arm was kept slightly abducted and flexed on elbow and wrist. Voluntary movements with this arm were lost and replaced by aimless movements and myoclonic jerks. Investigation of evoked potentials disclosed a slightly delayed N20 latency (21.2 ms, 18 ± 2 normal) on both sides, as well as a decreased N20-P25 component following stimulation of the left hand (0.5 μV, 1.7 right side, 4.9 ± 3.03 normal). Furthermore, investigation of long loop responses to sensory (median nerve) stimulation showed lost long latency responses on both sides, despite normal short latencies. At age 31 this patient described his right hand as odd. On examination this hand was clumsy and unable to imitate movements. Within a year the disease then progressed to a condition characterized by generalized rigidity with the neck kept extended, supranuclear palsies (severe dysphagia and dysarthria as well as staring gaze with a loss of conjugate eye movements), and myoclonus. At age 34 the patient is bedridden (posture in flexion at rest, decorticate following noxious stimulations) and dependent on caregivers. While unable to speak, he is able to communicate his emotions and needs by blinking.

Neuropathology

The brain of patient II-1 was fixed in 10% formalin and studied by conventional staining (cresyl violet, Spielmeyer's, Holzer's, PAS, oil red O, Perls') of slices cut from frozen blocks. Bodian's silver impregnation and tau immunocytochemistry were carried out on slices cut from paraffin- and paraplast-embedded blocks. The following anti-tau antibodies were used: AT8 (1:300, Innogenetics); AT180 (1:300, Innogenetics); AT100 (1:300, Innogenetics); PHF1 (1:100, gift from P. Davies); AD2 (1:500, gift from A. Delacourte); 12E8 (1:500, gift from P. Seubert); and Alz50 (1:100, gift from P. Davies). For ultrastructural investigation, formalin-fixed specimens of cingular cortex were washed in appropriate buffer, postfixed in 2.5% glutaraldehyde and 1% osmium tetraoxide, and embedded in epoxy resin. Semithin sections were stained with toluidine blue. Ultrathin sections were contrasted with lead citrate and uranyl acetate. Post-embedding tau immunostaining was carried out on ultrathin sections cut from additional non-osmicated specimens, which were etched with sodium periodate. An anti-tau polyclonal antibody A024 (1:20, Dako) was employed and revealed by goat anti-rabbit IgG conjugated to colloidal gold particles (Auroprobe GARG 10, Biocell). After immunolabeling, ultrathin sections were osmicated and contrasted.

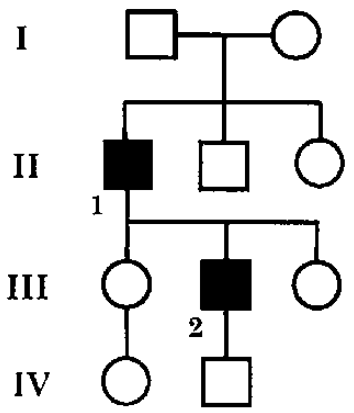

Fig. 1. The pedigree of family P.

DNA Analysis

DNAs of patients II-1 and III-2 were extracted from paraffin-embedded blocks of brain tissue (16) and peripheral leukocytes (17), respectively. Exon 10 of the tau gene was amplified by PCR and sequenced directly, as described (8). Primers from the intronic sequences flanking exon 10 (5'CGAGCAAGCAGCGGGTCC3' and 5'GTACGACTCACACCACTTCC3') were used to allow the exon 10 and the exon-intron boundaries to be examined. In some experiments amplified DNA was digested with MspI. Digestion products were run on 4% agarose gels and visualized by ethidium bromide staining.

Microtubule Assembly

Site-directed mutagenesis was used to change P301 to serine in the four-repeat 412 amino acid human tau isoform (in the numbering of the 441 amino acid isoform of human tau [18]) expressed from cDNA clone htau46. The construct was verified by DNA sequencing. Wild type and mutated tau proteins were expressed in *Escherichia coli* BL21(DE3) as described (19). Tau proteins were purified and their concentrations determined as described (20). Purified recombinant and mutated htau46 proteins (0.1 mg/ml, 2.3 μM) were incubated with bovine brain tubulin (1 mg/ml, 20 μM, Cytoskeleton) in assembly buffer at 37°C, as described (21). The assembly of tubulin into microtubules was monitored over time by a change in turbidity at 350 nm.

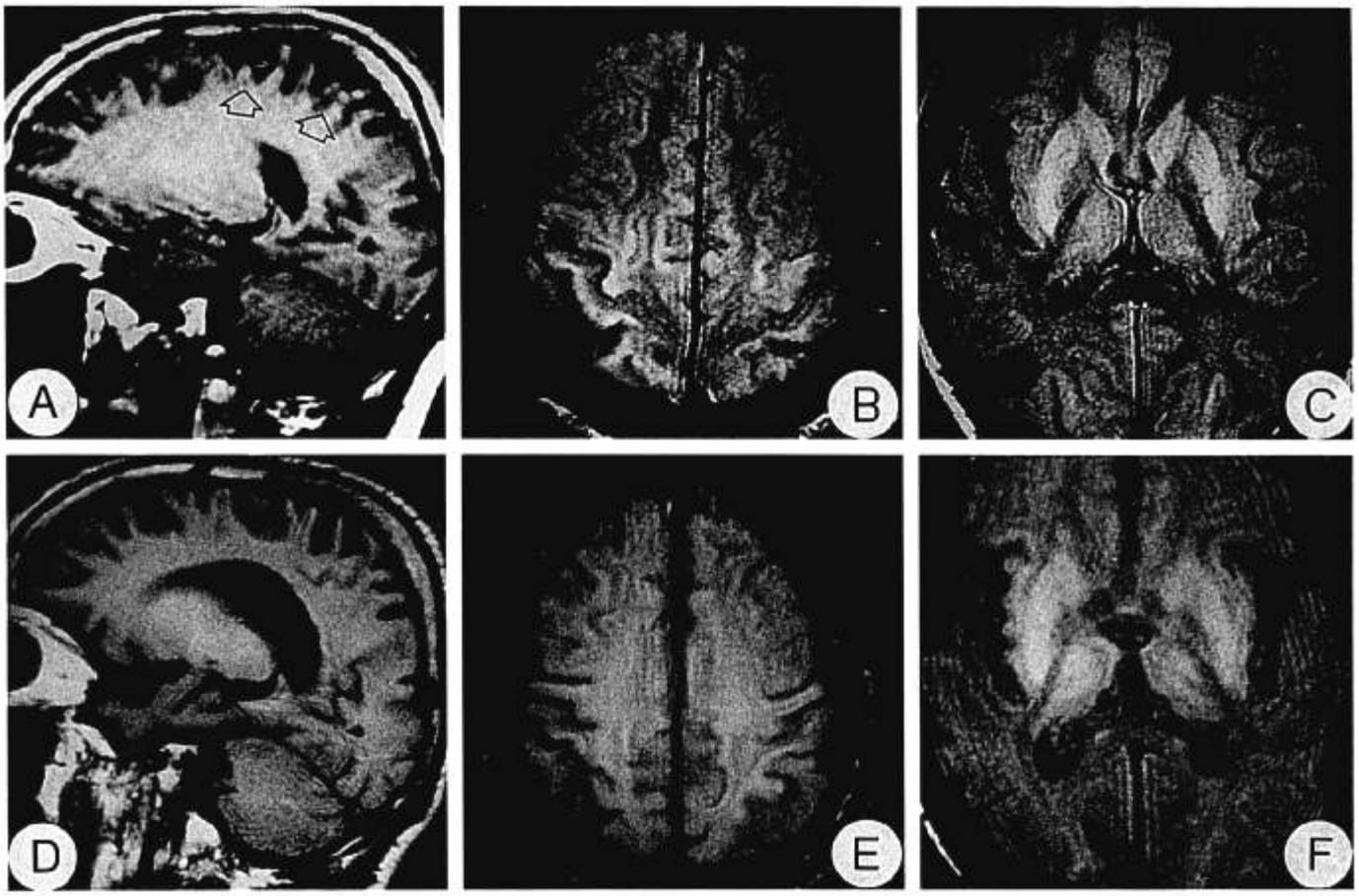

Fig. 2. Patient III-2. Two MRIs (A, B, C and D, E, F) illustrate the progression over 2 yr of the cerebral atrophy. The MRI (A, B, C), carried out when the patient was 32-yr-old, shows: (A) atrophy of the posterior frontal and the parietal regions (open arrows), as demonstrated by marked dilatation of the cortical sulci (right cerebral hemisphere, sagittal T1-weighted image), (B) increased signal intensity in the posterior frontal and the parietal cortices, more evident in the right hemisphere (left side in the figure) than in the left hemisphere (Spin-Echo, proton density image), and (C) dilatation of the right Sylvian fissure (left side in the figure) (Spin-Echo, proton density image). The MRI (D, E, F) shows that (D) the cortical atrophy has progressed to the anterior frontal and the temporal regions of the right cerebral hemisphere (sagittal T1-weighted image), (E) the cerebral cortex and subcortical white matter are involved on both sides, particularly at the frontoparietal level (Spin-Echo, proton density image), and (F) the dilatation of the Sylvian fissure is symmetrical (Spin-Echo, proton density image). The heads of caudate nuclei, putamina and thalami are remarkably hyperintense in both MRIs (C, F).

→

Fig. 3. Patient II-1, sections from frozen blocks of one cerebral hemisphere and the midbrain fixed in formalin. A, B and C: The frontal level, in which there is atrophy of the cortex and caudate nucleus, degeneration of the white matter (A, Spielmeyer's), overloading with sudanophilic lipids (B, oil red O), and subcortical fibrillary gliosis (C, Holzer's). D and E: The frontotemporal level shows atrophy of the caudate nucleus, shrinkage of mesial temporal structures and of the 2nd and 3rd temporal convolutions, shrinkage of the insula, normal myelin staining (D, Spielmeyer's), and lipid overloading in the internal capsule and the white matter of the cingular and temporal convolutions (E, oil red O). F, G and H: The parieto-occipital level illustrates a normal myelin staining (F, Spielmeyer's), lipid overloading in the white matter (G, oil red O), and subcortical gliosis (H, Holzer's). I and L (oil red O): Comparison of the lipid staining pattern of the white matter between the frontal lobe, in which a large number of scavenger cells is present (I, 270×), and the parietal and occipital lobes, in which scavenger cells are rare (L, 270×). M (Spielmeyer's) and N (oil red O): Degeneration of the frontopontine tract in the basal portion of midbrain. O: Increased iron-pigment content in the substantia nigra (Perls').

Fig. 4. Patient II-1. A and B: A semicircular argyrophilic inclusion in a cortical neuron and a Pick-body-like inclusion in a neuron of the basal nucleus (Bodian's, 633×). C and D: Adjacent sections of the cerebral cortex: Anti-tau antibody AT8 labels many more neurons than anti-tau antibody PHF1 (105×). E, F and G: Neuronal immunostaining patterns. Diffuse pattern with perinuclear enhancement (E, cortical neuron, AT8, 633×), diffuse pattern with enhancement next to the plasma membrane (F, cortical neuron, AT8, 633×), inclusion-body-like pattern (G, nigral neuron, PHF1, 633×). H, I and L: Glial involvement. A glial plaque in the occipital cortex (H, AT8, 422×), coiled bodies in the cerebellar white matter (I, AT8, 633×), and tufted astrocytes in the frontal white matter (L, AT8, 633×).

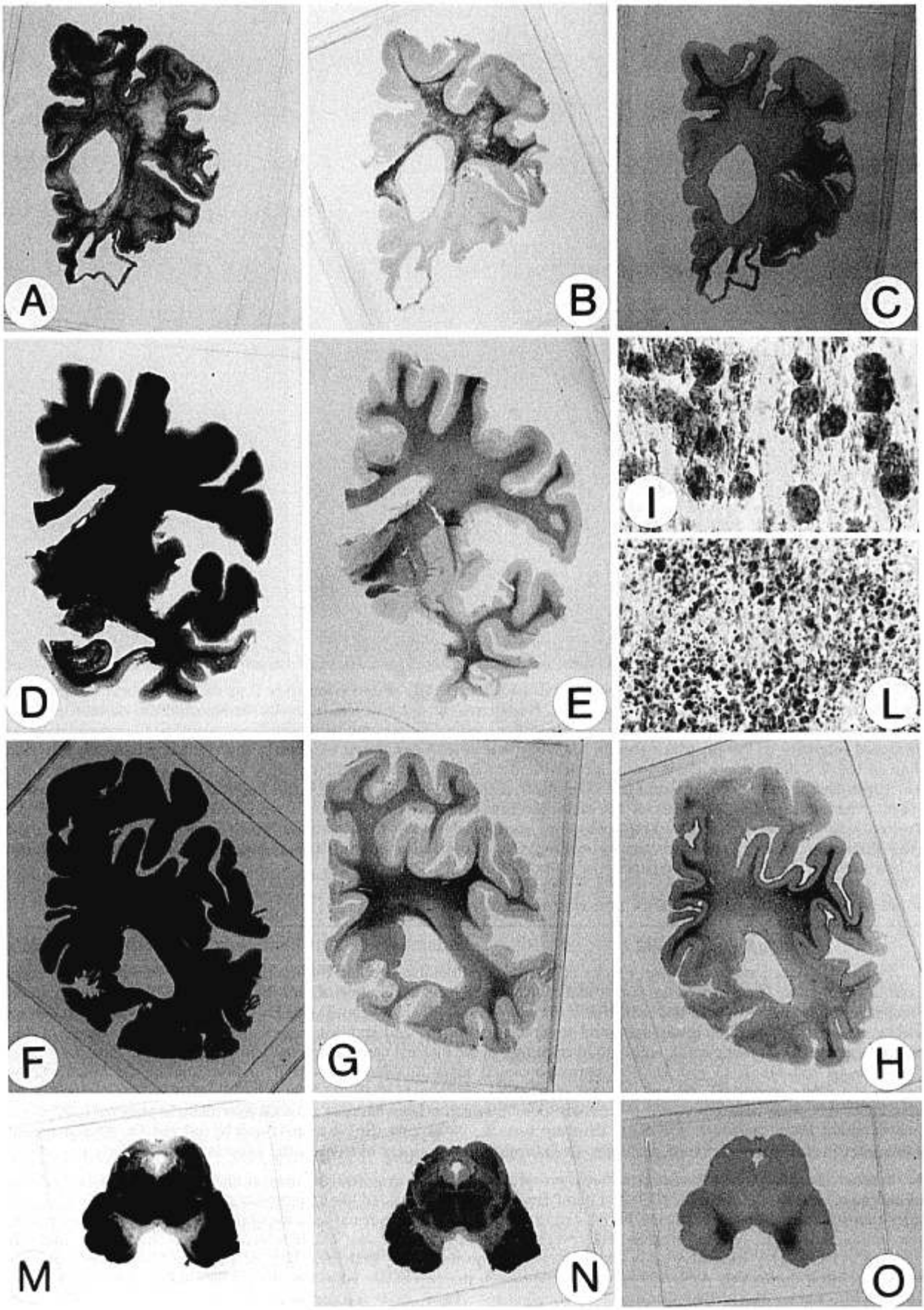

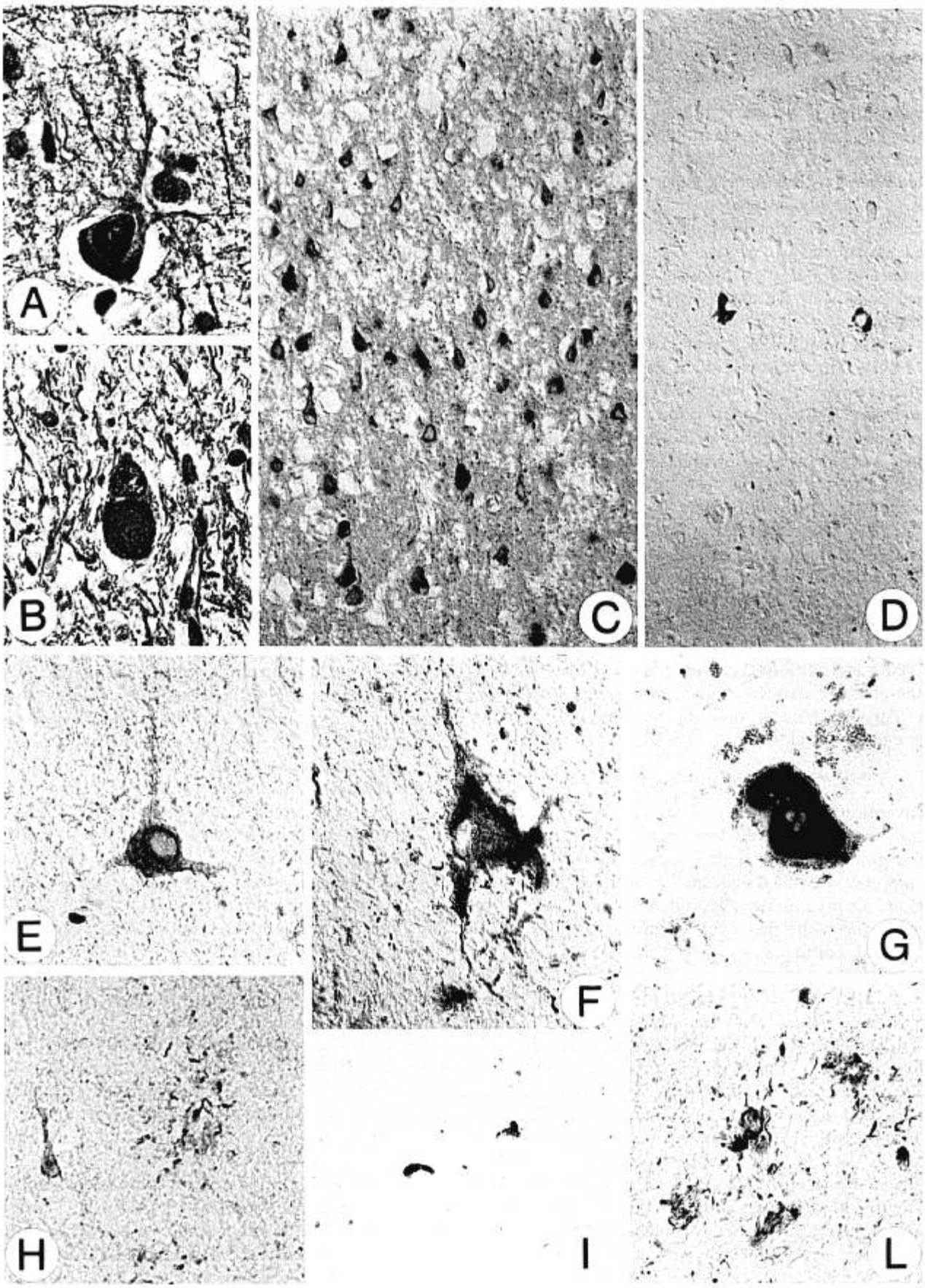

RESULTS

Gross Neuropathology of Patient II-1 and Comparison with MRI of Patient III-2

The necropsy of patient II-1 confirmed an earlier pneumoencephalographic investigation by showing atrophy of the brain (weight, 1,080 g) that was symmetrically distributed over the frontal and temporal lobes and over the insula. A knife-edge atrophy of the convolutions was present in the fronto-orbital regions. The atrophy also involved the subcortical white matter, the genu of corpus callosum and the heads of caudate nuclei, while sparing the rear portion of the upper temporal gyri and the Rolandic area.

At age 28 through 34, patient III-2 was investigated by 4 MRIs. They allowed the atrophy of the brain to be followed over time from the right parietal and adjacent frontal regions to the contralateral homologous regions, and subsequently to the temporal and insular regions, basal ganglia, and upper brainstem. The first 2 studies showed a slight cortical atrophy with signal hyperintensity in proton density and T2-weighted images in the right parietal region. One year later, the third MRI demonstrated that the parietal convolutions and the adjacent frontal cortex were asymmetrically shrunken (right more than left), and that signal hyperintensity was present in the atrophic cortex, subcortical white matter, both neostriata, and thalami (Fig. 2A–C). Five years after the first examination, an MRI showed that the atrophy also involved temporal and insular regions (Fig. 2D–F) and midbrain, as well as the heads of the caudate nuclei.

Light Microscopy

Conventional staining of slices from frozen blocks showed severe nerve cell loss, vacuolation and gliosis in the atrophic cortex, with layers II to IV being the most affected. Residual neurons in the inner layers were shrunken. Demyelination, spongiosis, and gliosis were present in the white matter of the prefrontal lobes (Fig. 3A, C) and could be followed through the midbrain along the frontopontine tracts (Fig. 3M, N). Most demyelinated areas were covered with lipid-laden, PAS-positive macrophages throughout (Fig. 3B, I). Other regions were less affected (Fig. 3D, F). However, droplets of sudanophilic lipids and gliosis were consistently present in white matter of several gyri (cingular, angular, temporal, and cuneatus), despite a normal myelin staining (Fig. 3E, G, H, L). Nerve cell loss and gliosis were marked in caudate nuclei, substantia nigra, and locus coeruleus, whereas they were mild in pallidum, putamen, tegmental gray, and bulbar olives. A slight cellular gliosis was present in thalamic nuclei, in the absence of neuronal loss. Iron-containing pigment was present in pallidum, subthalamic nucleus, and substantia nigra (pars reticulata) (Fig. 3O). The cerebellum appeared normal. Silver impregnation (Bodian's on paraplast-embedded blocks) occasionally disclosed small rod-like or semicircular inclusions in large and medium-sized neurons in the most preserved cortical areas (Fig. 4A), as well as Pick-body-like neuronal inclusions in pallidum, basal nucleus, thalamus, substantia nigra, and tegmental gray (Fig. 4B).

Immunocytochemistry

Abnormal staining for hyperphosphorylated tau was much more widespread than the pathological changes revealed by silver impregnation. Antibody AT8 (specific for phosphoserine 202 and phosphothreonine 205 of the protein [22]), antibody AT180 (specific for phosphothreonine 231 [23]), and antibody AT100 (specific for phosphothreonine 212 and phosphoserine 214 [24]) labeled most neurons in the cerebral cortex (following a fronto-occipital density gradient) (Fig. 4C), subcortical gray structures, brainstem, and cerebellar dentate nucleus. Pathological tau staining of pyramidal neurons and cells with round perikarya was finely granular and homogeneous, respectively. The staining was strong in either the perinuclear region or the region next to the cell membrane (Fig. 4E, F). In cortical neuropil and subcortical structures, these antibodies (AT8 and AT180 more than AT100) also stained axons, as well as dispersed and clustered grains and threads (Fig. 4F, H). The glial pathology was extensive and included both astrocytes and oligodendrocytes. Numerous tau-immunoreactive tufted astrocytes and coiled bodies were observed (Fig. 4H, I, L). The meshwork of immunolabeled cell processes was particularly dense in cerebral cortex, thalamus, molecular layer of hippocampus, and cerebellar dentate nucleus. This staining pattern differed from that obtained with anti-tau antibodies PHF1 and AD2 (both specific for phosphoserine 396 and phosphoserine 404 [25, 26]), which only stained 2%–3% of the AT8-positive cells (Fig. 4D). The immunoreactive structures had the morphology of elongated tangles and Pick-body-like inclusions. Large PHF1- and AD2-positive inclusions were observed in residual nigral neurons (Fig. 4G). Antibody 12E8 (specific for phosphoserine 262 and/or 356 [27]) labeled some neuronal inclusions, glial cells, and neuropil threads. Antibody Alz50, which recognizes a distinct conformation of tau when polymerized into filaments (28), labeled a few Pick-body-like inclusions.

Electron Microscopy

Perikarya and cell processes contained abundant abnormal filamentous structures (Fig. 5A–C). These structures appeared to be either single or paired, or (most often) packed into bundles. Widths ranged from 10 nm for single filaments to 30 nm for the thinnest bundles (Fig.

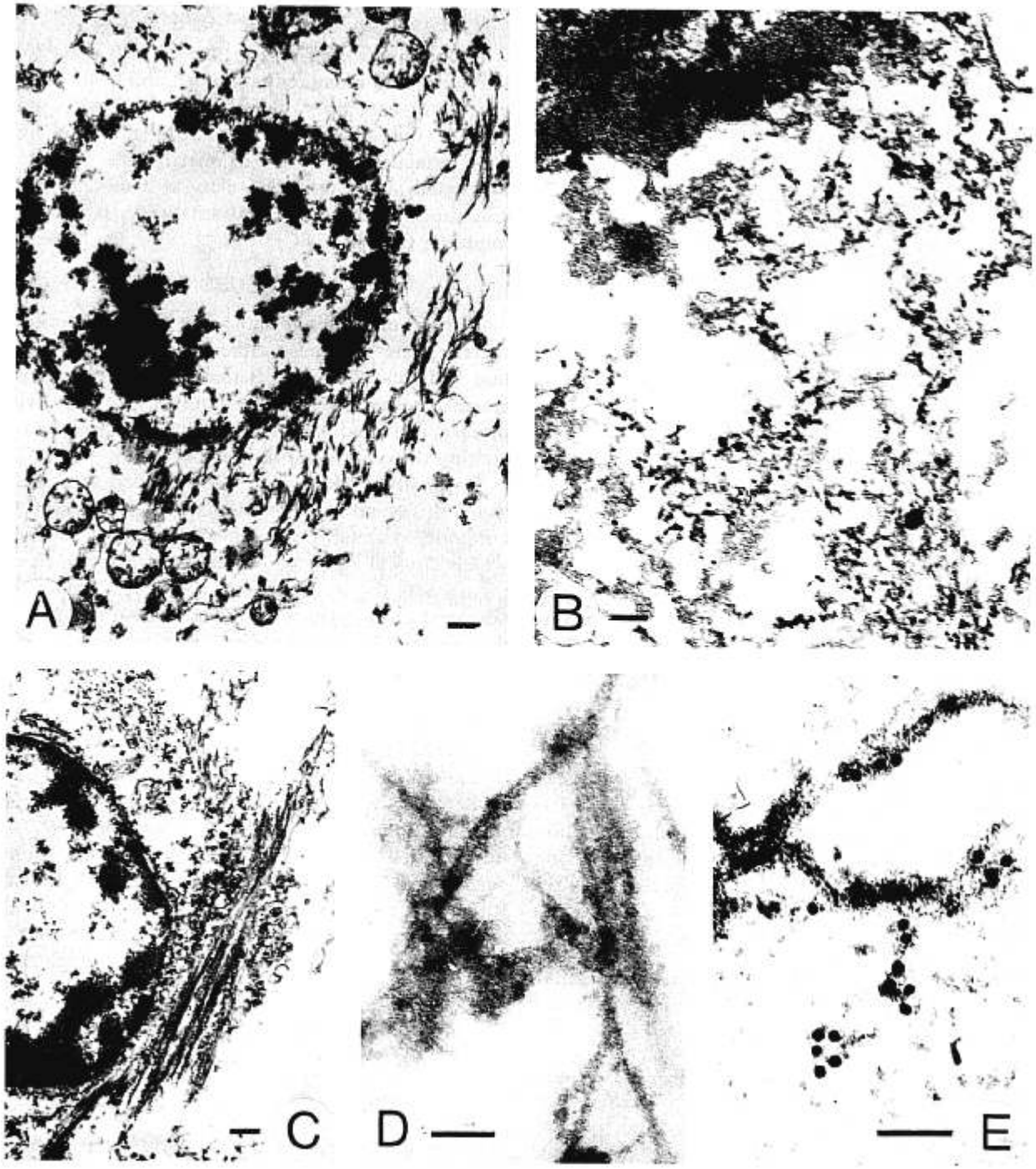

Fig. 5. Patient II-1: Ultrastructure of cells from the cingular cortex fixed in formalin and postfixed in glutaraldehyde. A, B and C: These cells exhibit intracytoplasmic abnormal filamentous structures that are either dispersed (A, bar, 400 nm) or packed in bundles (C, bar, 400 nm), and are decorated by gold particles (B, bar, 100 nm) after immunostaining with a polyclonal anti-tau antibody. D (bar, 100 nm): A high magnification reveals that relatively dispersed abnormal filaments often appear paired. E (bar, 100 nm): 10-nm gold decoration shows that the width of thinner filaments is comparable with the diameter of gold particles.

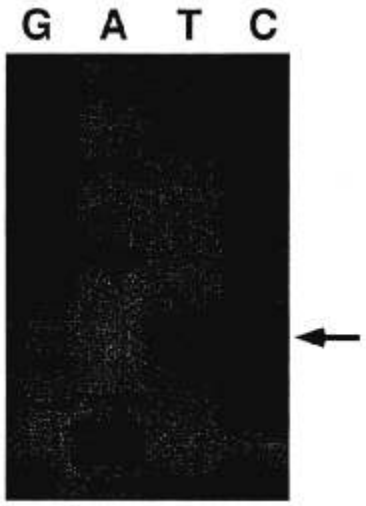

Fig. 6. DNA sequencing of exon 10 from genomic DNA of Patient III-2. The arrow aims at a T nucleotide in addition to the normal C nucleotide.

5D). These structures appeared to be straight, since no clear-cut twisting was observed. The filaments were decorated by gold particles, revealing staining with the anti-tau polyclonal antibody A024 (Fig. 5B, E). In semithin sections, this antibody labeled neurons, glial cells, and their processes.

DNA Sequence Analysis

Sequencing of exon 10 and of intronic sequences flanking exon 10 of the tau gene in patients II-1 and III-2 identified a C to T transition in the first base of codon 301 (Fig. 6), which leads to a predicted proline to serine substitution at position 301 (P301S). This substitution removes an MspI restriction site which allowed confirmation of the mutation in both patients (Fig. 7). The mutation was not found in 50 controls.

Microtubule Assembly

Recombinant four-repeat htau46 with the P301S mutation showed a markedly reduced ability to promote microtubule assembly, when compared with wild-type htau46 (Fig. 8B). Thus, the P301S mutation led to an 80% reduction in the rate of microtubule assembly when expressed as the optical density at 2 min. However, the magnitude of the effect was smaller than for the P301L mutation (20) (Fig. 8C).

DISCUSSION

The present findings show that the P301S mutation in the tau gene can cause either FTD or CBD, suggesting that FTD and CBD are distinct clinical phenotypes of a single disease. This disease could be equated with Pick disease, provided that the latter is one disease entity overarching different lobar atrophies (1, 29).

Originally, Pick disease was regarded as a disease entity with several anatomo-clinical phenotypes (i.e. frontal, temporal, parietal, occipital, and striatal), depending on which clinical signs were present and on which cerebral region was the most atrophic (30). The frontal and the temporal phenotypes were the most common (31–33). As the nosography and the diagnostic criteria for Pick disease have evolved over the years, the disease in patient II-1 could have been given at least 3 different diagnoses. Pick disease would have been the first choice because of the marked atrophy of the frontal and temporal lobes and of the caudate nuclei, the degeneration of long association (to the occipital cortex) and projection (to the pontine gray) bundles originating in frontal and temporal cortices, and the preservation of selected convolutions, in particular a portion of the upper temporal gyrus and the Rolandic region. However, a diagnosis of Pick disease would have been ruled out if the presence of Pick bodies had been considered a necessary morphological feature.

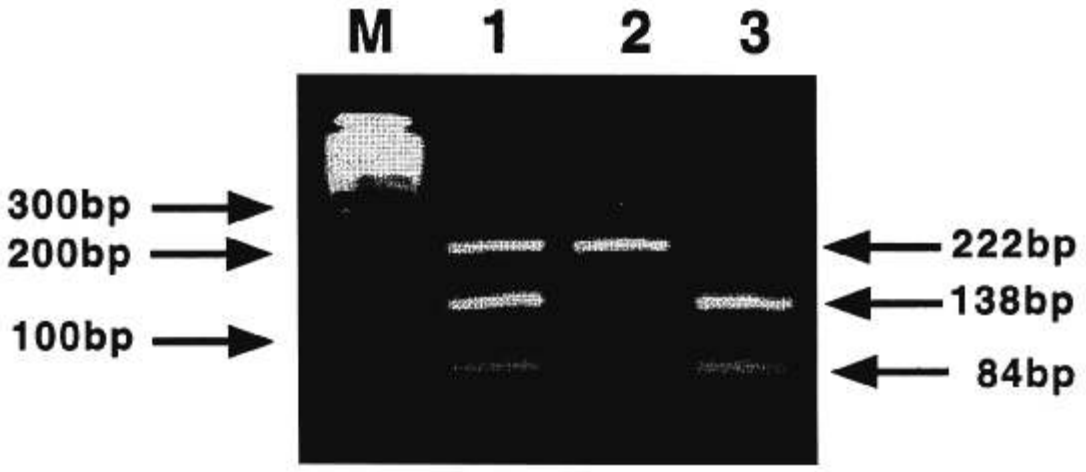

Fig. 7. MspI digestion products of amplified exon 10 showing a band at 222 bp in lanes 1 and 2. The marker is a 100-bp ladder. Lane 1 is exon 10 from Patient II-1. Lane 2 is exon 10 from Patient III-2. Lane 3 is exon 10 from a healthy individual.

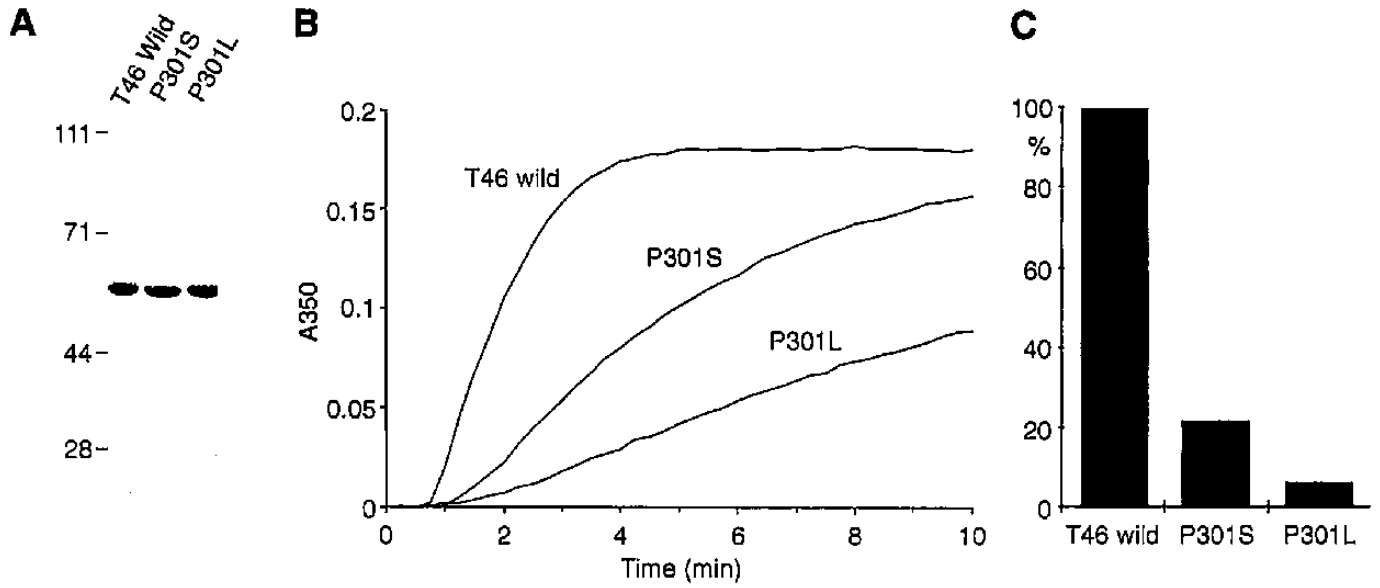

Fig. 8. Effects of the P301S mutation on the ability of four-repeat htau46 (412 amino acid isoform of human tau) to promote microtubule assembly. Comparison with the P301L mutation. A: Coomassie-stained SDS-PAGE of purified recombinant htau46, htau46P301S, and htau46P301L. B: Polymerisation of tubulin induced by wild-type htau46, htau46P301S and htau46P301L, as monitored over time by turbidimetry. C: Optical densities for wild-type htau46 and the 2 mutants at 2 min (expressed as % of wild-type htau46, taken as 100%). Amino acid numbering is according to the 441 amino acid isoform of human tau.

of Pick disease (34, 35). In fact, patient II-1 had only small numbers of argyrophilic inclusions and no obvious Pick bodies in cortical regions, particularly the hippocampus. On this basis, a diagnosis of non-Alzheimer, non-Pick frontal lobe degeneration would have been the most likely (36). Actually, the disease of patient II-1 can be regarded as part of the spectrum of FTDP-17 dementias (3, 5), as these dementias have been recognized as a discrete entity characterized by mutations in the tau gene with filamentous tau pathology in neurons and glial cells, and frontotemporal atrophy.

In contrast to patient II-1, a diagnosis of CBD would have been made in patient III-2, based on clinical presentation (14, 37), early MRI findings, and neurophysiological findings (38, 39), which indicated that the telencephalic sensory and motor structures were involved asymmetrically. The relationship between CBD and Pick disease has been questioned, since CBD clinically mimics the parietal phenotype of Pick disease (40, 41). However, by neuropathological criteria, CBD and Pick disease are considered to be distinct disease entities (35), although controversial cases have been reported (42). Serial MRIs carried out in patient III-2 showed that brain atrophy had extended over the years to frontal and temporal regions and heads of caudate nuclei, which had been affected in patient II-1 since the beginning of the disease.

The present results suggest that it is essential for an interpretation of genotype-phenotype correlations and of pathological findings not to be too stringent when reviewing the nosography of lobar atrophies with mutations in the tau gene. The finding that such different clinical presentations as FTD and CBD can be associated with the same mutation in the tau gene points to genetic background as an important factor influencing the vulnerability of particular neurons and glial cells. In our patients it appears to determine whether cell degeneration starts in frontotemporal or parietal cortical areas, and along which pathways it develops.

Additional findings also point to phenotypic heterogeneity when this family is compared with other FTDP-17 families. Thus, hyperintensity of neostriatum and thalamus was found by MRI in patient III-2. It is a characteristic of Creutzfeldt-Jakob disease (43), possibly reflecting glial cell proliferation and overloading with aggregated protein. Moreover, patient II-1 showed antibody-staining peculiarities that have so far not been described. Thus, not only were there many more cells immunoreactive with anti-tau antibody AT8 than with antibodies PHF1 or AD2, but also the AT8 staining was diffuse and granular, whereas staining with PHF1, AD2, and Alz50 was Pick-body-like. The heterogeneous phosphorylation of the abnormal tau in different cell populations might have been related to the localization or the nature of the mutation in this family. Finally, sudanophilic lipids and subcortical gliosis were detected in the hemispheric white matter in patient II-1. In some areas, they occurred in the absence of cortical atrophy or Wallerian degeneration, possibly pointing to glial cell involvement as the first lesion in these regions.

In adult human brain, 6 tau isoforms are produced from a single gene by alternative mRNA splicing (13, 18). They differ from each other by the presence or absence

of 29- or 58-amino acid inserts located in the amino-terminal half, and a 31-amino acid repeat located in the C-terminal half. Inclusion of the latter, which is encoded by exon 10 of the tau gene, originates the 3 tau isoforms with 4 repeats each (44). The other 3 isoforms have 3 repeats each. The repeats and some adjoining sequences constitute the microtubule-binding domains of tau protein. The P301S mutation is located in exon 10, thus only affecting four-repeat tau isoforms. Two other mutations have been described in exon 10. The N279K mutation has been reported in 2 families thus far (10, 11), whereas the P301L mutation is much more common (6, 7, 9, 12). Both mutations lead to the formation of twisted ribbon-like filaments consisting predominantly of four-repeat tau isoforms (12, 45, 46). The EM results on the P301S mutation reported here are consistent with these findings, although twisting of the filaments has not been demonstrated in the autopsy material thus far. It may require the extraction of isolated dispersed filaments. The other known mutations in *tau* are either missense mutations located outside exon 10 or intronic mutations located close to the splice-donor site of the intron following exon 10, where they disrupt a predicted stem-loop structure (7, 8, 47). Missense mutations located outside exon 10 lead to a tau pathology, which cannot be distinguished from that of Alzheimer disease (48). The intronic mutations lead to the formation of wide twisted ribbons made of four-repeat tau isoforms in both neurons and glial cells (49).

The age of onset of the disease in this family with the P301S mutation is in the third decade, contrasting with the much later age of onset in families with the P301L mutation. Moreover, the total amount of tau pathology is larger in the former than in the families with the P301L mutation examined thus far (12, 45). The reasons for these differences are unknown. Biochemically, recombinant tau with the P301S mutation showed a reduced ability to promote microtubule assembly, although this effect was smaller than for the P301L mutation (20). One distinguishing feature of the P301S mutation is that it creates a potential new phosphorylation site. Phosphorylation of this residue in the second microtubule-binding domain might lead to a reduced ability of tau to promote microtubule assembly and to bind to microtubules. This phenomenon could significantly contribute to the early age of onset of the disease and the widespread tau pathology associated with this mutation. It also argues in favor of a direct relationship between the age of onset and the number of neurons and glial cells with pathological tau.

REFERENCES

1. Neary D, Kertesz A, Hachinski V. Frontotemporal dementia, Pick disease, and corticobasal degeneration. One Entity or 3? Arch Neurol 1997;54:1425–29
2. Mann DMA. Dementia of frontal type and dementias with subcortical gliosis. Brain Pathol 1998;8:325–38
3. Foster NL, Wilhelmsen K, Sima AAF, Kones MZ, D'Amato CJ, Gilman S, and Conference Participants. Frontotemporal dementia and parkinsonism linked to chromosome 17: A consensus conference. Ann Neurol 1997;41:706–15
4. Wilhelmsen KC, Lynch T, Pavlou E, Higgins M, Nygaard TG. Localization of disinhibition-dementia-Parkinsonism-amyotrophy complex to 17q21–22. Am J Hum Genet 1994;55:1159–65
5. Spillantini MG, Bird TD, Ghetti B. Frontotemporal dementia and parkinsonism linked to chromosome 17: A new group of tauopathies. Brain Pathol 1998;8:387–402
6. Poorkaj P, Bird TD, Wijsman E, et al. Tau is a candidate gene for chromosome 17 frontotemporal dementia. Ann Neurol 1998;43:815–25
7. Hutton M, Lendon CL, Rizzu P, et al. Association of missense and 5′-splice-site mutations in tau with the inherited dementia FTDP-17. Nature 1998;393:702–5
8. Spillantini MG, Murrell JR, Goedert M, Farlow MR, Klug A, Ghetti B. Mutation in the tau gene in familial multiple system tauopathy with presenile dementia. Proc Natl Acad Sci USA 1998;95:7737–41
9. Dumanchin C, Camuzat A, Campion D, et al. Segregation of a missense mutation in the microtubule-associated protein tau gene with familial frontotemporal dementia and parkinsonism. Hum Mol Genet 1998;7:1825–9
10. Clark LN, Poorkaj P, Wszolek Z, et al. Pathogenic implications of mutations in the tau gene in pallido-ponto-nigral degeneration and related neurodegenerative disorders linked to chromosome 17. Proc Natl Acad Sci USA 1998;95:13103–7
11. Delisle MB, Murrell JR, Richardson R, et al. A mutation at codon 279 (N279K) in exon 10 of the *tau* gene causes a tauopathy with dementia and supranuclear palsy. Acta Neuropathol 1999 (in press)
12. Mirra SS, Murrell JR, Gearing M, et al. Tau pathology in a family with dementia and a P301L mutation in *tau*. J Neuropathol Exp Neurol 1999;58:335–45
13. Spillantini MG, Goedert M. Tau protein pathology in neurodegenerative diseases. Trends Neurosci 1998;21:428–33
14. Rinne J, Lee M, Thompson P, Marsden C. Corticobasal degeneration. A clinical study of 36 cases. Brain 1994;117:1183–98
15. Gallien P, Verin M, Rancurel G, De Marco O, Edan G. First familial cases of cortico-basal degeneration. (Abstract) Neurology 1998;50(Suppl. 4):S65.004
16. Nichols WC, Gregg RE, Brewer HB, Benson MD. A mutation in apolipoprotein A-1 in the Iowa type of familial amyloidotic polyneuropathy. Genomics 1990;8:318–23
17. Madison L, Hoar DI, Holroyd CD, Crisp M, Hodes ME. DNA banking: The effect of storage of blood and isolated DNA on the integrity of DNA. Am J Med Genet 1987;27:379–90
18. Goedert M, Spillantini MG, Jakes R, Rutherford D, Crowther RA. Multiple isoforms of human microtubule-associated protein tau: Sequences and localization in neurofibrillary tangles of Alzheimer's disease. Neuron 1989;3:519–26
19. Goedert M, Jakes R. Expression of separate isoforms of human tau protein: Correlation with the tau pattern in brain and effects on tubulin polymerisation. EMBO J 1990;9:4225–30
20. Hasegawa M, Smith MJ, Goedert M. Tau proteins with FTDP-17 mutations have a reduced ability to promote microtubule assembly. FEBS Lett 1998;437:207–10
21. Hasegawa M, Crowther RA, Jakes R, Goedert M. Alzheimer-like changes in microtubule-associated protein tau induced by sulfated glycosaminoglycans. Inhibition of microtubule binding, stimulation of phosphorylation and filament assembly depend on the degree of sulfatation. J Biol Chem 1997;272:33118–24
22. Goedert M, Jakes R, Vanmechelen E. Monoclonal antibody AT8 recognizes tau protein phosphorylated at both serine 202 and threonine 205. Neurosci Lett 1995;189:167–70

23. Goedert M, Jakes R, Crowther RA, et al. Epitope mapping of monoclonal antibodies to the paired helical filaments of Alzheimer's disease: Identification of phosphorylation sites in tau protein. Biochem J 1994;301:871–77
24. Zheng-Fischhöfer Q, Biernat J, Mandelkow EM, Illenberger S, Godemann R, Mandelkow E. Sequential phosphorylation of tau by glycogen synthase kinase-3β and protein kinase A at Thr212 and Ser214 generates the Alzheimer-specific epitope of antibody AT100 and requires a paired-helical-filament-like conformation. Eur J Biochem 1998;252:542–52
25. Otvos L, Feiner L, Lang E, Szendrei GI, Goedert M, Lee VM-Y. Monoclonal antibody PHF-1 recognizes tau protein phosphorylated at serine residues 396 and 404. J Neurosci Res 1994;39:669–73
26. Buée-Scherrer V, Condamines O, Mourton-Gilles C, et al. AD2, a phosphorylation dependent monoclonal antibody directed against tau proteins found in Alzheimer's disease. Mol Brain Res 1996;39: 79–88
27. Seubert P, Mawal-Dewan M, Barbour R, et al. Detection of phosphorylated Ser262 in fetal tau, adult tau and paired helical filament tau. J Biol Chem 1995;270:18917–22
28. Carmel G, Mager EM, Binder LI, Kuret J: The structural basis of monoclonal antibody Alz50's selectivity for Alzheimer's disease pathology. J Biol Chem 1996;271:32789–95
29. Kertesz A, Hudson L, Mackenzie IR, Munoz DG. The pathology and nosology of primary progressive aphasia. Neurology 1994;44: 2065–72
30. Jervis GA. Pick's disease. In: Minkler J, ed. Pathology of the Nervous System. New York: McGraw-Hill 1971, vol. 2: 1395–404
31. Spatz H. La maladie de Pick, les atrophies systématisées progressives et la sénescence cérébrale prématurée localisée. Proc. 1st Int. Cong. Neuropathol. (Rome, Sept. 8–13, 1952) Torino: Rosenberg & Sellier 1952, vol. 2:375–406
32. Escourolle R. La maladie de Pick. Étude critique d'ensemble et synthèse anatomoclinique. Paris: Foulon, 1956
33. Tissot R, Constantinidis J, Richard J. La maladie de Pick. Paris: Masson, 1975
34. Litvan I, Hauw JJ, Bartko JJ, et al. Validity and reliability of the preliminary NINDS neuropathologic criteria for progressive supranuclear palsy and related disorders. J Neuropathol Exp Neurol 1996;15:223–31
35. Dickson D. Pick's disease: A modern approach. Brain Pathol 1998;8:339–354
36. Brun A, Englund A, Gustafson L, et al. Clinical and neuropathological criteria for frontotemporal dementia. J Neurol Neurosurg Psychiat 1994;57:416–18
37. Litvan I, Agid Y, Goetz C, et al. Accuracy of the clinical diagnosis of corticobasal degeneration: A clinicopathologic study. Neurology 1997;48:119–25
38. Carella F, Ciano C, Panzica F, Scaioli V. Myoclonus in corticobasal degeneration. Mov Disord 1997;12:598–603
39. Grisoli M, Fetoni V, Savoiardo M, Girotti F, Bruzzone MG. MRI in corticobasal degeneration. Eur J Neurol 1995;2:547–52
40. Cambier J, Masson M, Dairou R, Henin D. Étude anatomo-clinique d'une forme pariétale de Maladie de Pick. Rev Neurol (Paris) 1981;137:33–38
41. Lang AE, Bergeron C, Pollanen MS, Ashby P. Parietal Pick's disease mimicking cortical-basal ganglionic degeneration. Neurology 1994;44:1436–40
42. Jendroska K, Rossor MN, Mathias CJ, Daniel SE. Morphological overlap between corticobasal degeneration and Pick's disease: A clinicopathologic report. Mov Disord 1995;10:111–14
43. Finkenstaedt M, Szudra A, Zerr I, et al. MR Imaging of Creutzfeldt-Jakob disease. Radiology 1996;199:793–98
44. Goedert M, Spillantini MG, Potier MC, Ulrich J, Crowther RA. Cloning and sequencing of the cDNA encoding an isoform of microtubule-associated protein tau containing four tandem repeats: differential expression of tau protein mRNAs in human brain. EMBO J 1989;8:393–99
45. Spillantini MG, Crowther RA, Kamphorst W, Heutink P, Van Swieten JC. Tau pathology in two Dutch families with mutations in the microtubule-binding region of tau. Am J Pathol 1998;153:1359–63
46. Reed LA, Schmidt ML, Wszolek ZK, et al. The neuropathology of a chromosome 17-linked autosomal dominant parkinsonism and dementia (pallido-ponto-nigral degeneration). J Neuropathol Exp Neurol 1998;57:588–601
47. Goedert M, Crowther RA, Spillantini MG. Tau mutations cause frontotemporal dementias. Neuron 1998;21:955–58
48. Spillantini MG, Crowther RA, Goedert M. Comparison of the neurofibrillary pathology in Alzheimer's disease and familial presenile dementia with tangles. Acta Neuropathol 1996;92:42–48
49. Spillantini MG, Goedert M, Crowther RA, Murrell JR, Farlow MJ, Ghetti B. Familial multiple system tauopathy with presenile dementia: A disease with abundant neuronal and glial tau filaments. Proc Natl Acad Sci USA 1997;94:4113–18

Received November 30, 1998
Revision received March 4, 1999
Accepted March 8, 1999